Advances in Science and Technology Research Journal

Advances in Science and Technology Research Journal, 18(6), 351–360
https://doi.org/10.12913/22998624/191955
ISSN 2299-8624, License CC-BY 4.0

Received: 2024.07.23
Accepted: 2024.08.15
Published: 2024.09.08

Influence of Abrasive Waterjet Parameters on Surface Quality and Material Removal in WNiFe Tungsten Alloy

Lisa Dekster[1]

[1] Department of Manufacturing Systems, Faculty of Mechanical Engineering and Robotics, AGH University of Krakow, 30-059 Cracow, Poland
E-mail: dekster@agh.edu.pl

ABSTRACT

Abrasive Waterjet (AWJ) milling effectively processes high-strength materials like WNiFe tungsten alloy without altering their properties. This study investigates the effects of jet pressure, traverse speed, and abrasive mass flow rate on the machining performance. The results indicate that increasing jet pressure significantly enhances groove depth, with higher pressures leading to more aggressive material removal. Conversely, higher traverse speeds reduce groove depth, emphasizing the need for slower speeds for deeper penetration. Increased abrasive mass flow rates also significantly improve groove depth but pose challenges related to material wear and cost. Surface analysis using scanning electron microscopy (SEM) revealed that higher jet pressures and lower traverse speeds produce smoother surfaces and more distinct grooves. The findings highlight the importance of optimizing AWJ parameters to achieve efficient material removal and desired groove geometries. This research provides valuable insights for improving AWJ machining of tungsten alloys in industrial applications.

Keywords: diagnostics, failure detection, rolling stock, railway track, railway, railway wheel, railway bogie, railway failure.

INTRODUCTION

Abrasive Waterjet milling is a versatile technique for processing high-strength materials without altering their properties [1]. It is effective for milling intricate geometries in hard-to-cut materials such as Hastelloy C-276 and 7075-T6 aluminum alloy [1, 2]. The process parameters, including waterjet pressure, traverse rate, and abrasive flow rate, directly influence the material removal rate and surface roughness [1, 3]. Optimization techniques, such as response surface methodology, help determine the ideal parameter combinations for high productivity and surface quality [1]. AWJ technology can cut various materials, including ceramics and hard materials like carbides and PCD, though it presents challenges in controlling erosion rates and predicting outcomes [4, 5].

Previous studies, particularly by Kong et al. [6] and Huang et al. [7], have emphasized the role of microstructure in erosion mechanisms during plain waterjet (WJ) processes. These studies highlight phenomena such as plastic deformation and intergranular cracks, indicating material removal. Hlaváček et al. [8] discussed the influence of microstructure on the surface integrity of workpieces during AWJ cutting. Research findings indicate that AWJ cutting causes plastic deformation of grains, leading to notch cavities on the cut surface. The characteristics and quantity of these notch cavities, as well as the deposition of nanometer-sized aggregate particles, are influenced by controlling the cutting speed [9]. During AWJ machining, the metal surface experiences severe plastic deformation due to repeated abrasive particle impacts. This deformation can alter the subsurface microstructure, thereby affecting wear and tribological properties [10].

Tungsten heavy alloys (WHA), such as WNiFe, are promising alternatives to pure

tungsten due to their machinability and excellent mechanical properties [11, 12]. They are used in environments subjected to extreme conditions, such as plasma-facing components in nuclear fusion reactors [11, 14]. WNiFe alloys also improve the performance and lifespan of high-pressure die-casting tools [13]. These alloys, with high tungsten content, are ideal for military applications due to their density, wear resistance, and high-temperature stability [15]. They maintain structural integrity under high heat flux without macroscopic failure [14]. The WNiFe tungsten alloy is utilized in various specialized applications due to its unique properties. Specifically, it is used in military equipment for armour-piercing ammunition and kinetic energy penetrators. In the aerospace sector, it serves as a counterweight in aircraft components. Additionally, WNiFe alloys are employed in the medical field for radiation shielding and in nuclear applications for similar shielding purposes. Due to the properties, machining this tungsten alloy poses a challenge. Researching its feasibility for efficient cutting is crucial. The impact toughness of the alloy is influenced by the microstructure, with swaging leading to changes in the shape of tungsten grains and increased tungsten contiguity, affecting impact failure behaviour [16].

Kumar, Sreebalaji, and Pridhar [17] optimized AWJ machining parameters for aluminum/tungsten carbide composites, focusing on stand-off distance, traverse speed, and tungsten carbide percentage. They found that transverse speed and tungsten carbide percentage significantly influenced the material removal rate and surface roughness. Yan Wang et al. [18] studied the cutting of tungsten plates for fusion devices using a premixed AWJ, demonstrating that transverse speed significantly impacts surface roughness. Reducing transverse speed decreased surface roughness while increasing jet pressure improved the cut's depth. Derzija Begic-Hajdarevic and Izet Bijelonja [19] explored laser beam machining of tungsten alloy, focusing on the heat-affected zone (HAZ). They found larger HAZ in thinner plates and detected microcracks at the HAZ borders. Wang, Wang, and Zhan [20] modelled AWJ parameters for cutting rolled tungsten plates, relevant for constructing tokamaks. They used multivariate nonlinear regression and backpropagation ANN models to predict surface roughness, finding that slower cutting speeds and higher jet pressures significantly improve surface quality. Topological parameters like surface roughness (Ra, Rz), skewness (Rsk), and kurtosis (Rku) are essential for understanding tribological properties and wear behaviour. Studies such as Karkalos, Muthuramalingam, and Karmiris-Obratański [21] highlight their importance in predicting wear performance. While our research primarily examines the impact of AWJ parameters on material removal and surface integrity, the relevance of surface topography in determining tribological properties aligns with existing literature.

From the literature review, it is clear that a comprehensive study on AWJ machining of tungsten alloys, especially WNiFe, is lacking. This work conducts an experimental study with varying jet pressure, traverse speed, and abrasive mass flow rate. Statistical analysis is performed on results such as depth of penetration and kerf taper angle to determine their correlation with input parameters and the relative importance of these parameters.

MATERIALS AND METHODS

This study utilized a tungsten heavy alloy consisting of 92.5% tungsten (W), 5.25% nickel (Ni), and 2.25% iron (Fe). The microstructure of the WNiFe alloy consists of tungsten grains embedded in a nickel-iron matrix. Tungsten precipitates within the matrix further enhance the alloy's properties. This two-phase composite structure, with tungsten as the reinforcement phase and the nickel-iron matrix providing ductility, is critical for the alloy's mechanical behaviour.

The WNiFe alloy exhibits high ultimate tensile strength and low elongation, primarily due to the high fraction of tungsten cleavage planes and high-density dislocations in both the tungsten grains and the matrix phase. These dislocations hinder the movement of dislocation lines, increasing the material's yield strength. The alloy's thermal stability and wear resistance also make it suitable for extreme environments, such as aerospace, defence, and nuclear industries. The combination of tungsten's hardness and the ductility of the nickel-iron matrix allows the alloy to withstand high mechanical loads and resist deformation under stress.

The experiments were conducted on an HWE-1520 RIDDER Automatisierungs GmbH machine (H.G. RIDDER H., Hamm, Germany). This machine supports various jet pressure values

(50 to 400 MPa), abrasive mass flow rates (10 to 600 g/min), and traverse feeds. It is operated using Siemens SINUMERIK software, which allows precise control over the machining parameters. For this study, the specific parameters varied are shown in Table 1.

The abrasive used was garnet with a mesh size of #80. The nozzle diameter was 1 mm. Preliminary experiments were conducted to establish a suitable range for the machining parameters, ensuring that the selected parameters could effectively evaluate the machinability of the tungsten alloy and the geometric characteristics of the machined grooves. The Box-Behnken design was chosen for the experimental plan due to its efficiency in terms of the number of experiments required. This design allows for the assessment of the main effects and interactions of the process parameters while minimizing the total number of experiments, thereby reducing costs. The Box-Behnken design is particularly advantageous for fitting quadratic response surfaces and constructing second-order polynomial models, making it suitable for this type of experimental optimization. In this study, 15 experimental runs were conducted, which is adequate to assess the effects of the selected parameters on machining performance. Figure 1 illustrates the cutting method and the sample in a graphical representation. Slot dimensions were measured using a VHX-7000 ultra-deep-field microscope (KEYENCE, Mechelen, Belgium). This focus variation microscope (FVM) utilizes 20–2000× lenses and a white light LED source to achieve high-resolution 3D surface measurements. The resulting images had a 4096 × 2160 pixel resolution, enabling precise kerf angle and depth measurements. Figure 2 shows the incision profile to better understand the measuring method.

Images were acquired using the Phenom XL scanning electron microscope (SEM), which provides high-resolution imaging essential for detailed sample analysis. The Phenom XL, equipped with a four-segment backscattered electron detector, enables the capture of sharp images with chemical composition contrast. This SEM can examine samples up to 100×100×65 mm in size and features a streamlined loading mechanism that allows for rapid image acquisition, typically within 60 seconds. These images were utilized to assess the surface quality and to elucidate the mechanisms of material removal by abrasive particles during the machining process.

Table 1. Experimental parameters

Levels	Jet pressure [MPa]	Feed rate [mm/min]	Abrasive mass flow rate [g/s]	Stand-off distance [mm]
1	150	150	2	2
2	200	225	3	
3	250	300	4	

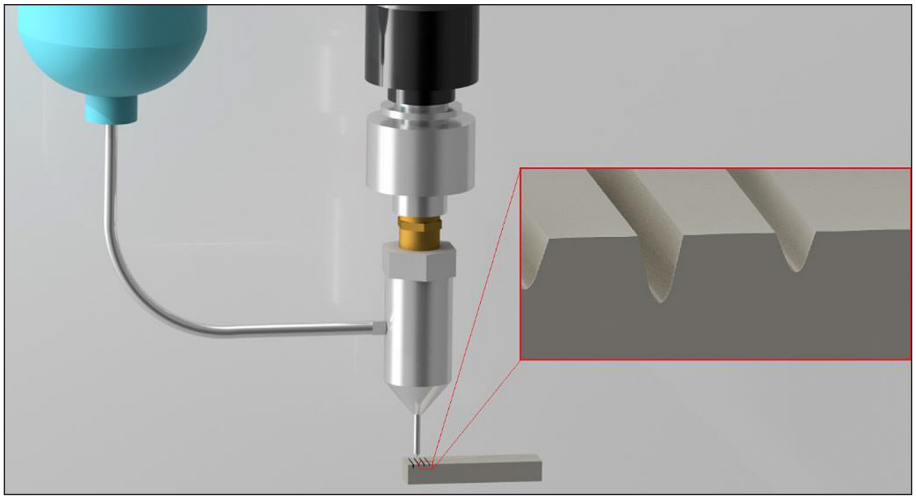

Figure 1. Graphical representation of the AWJM process and the influence of the process parameters on the groove's geometry

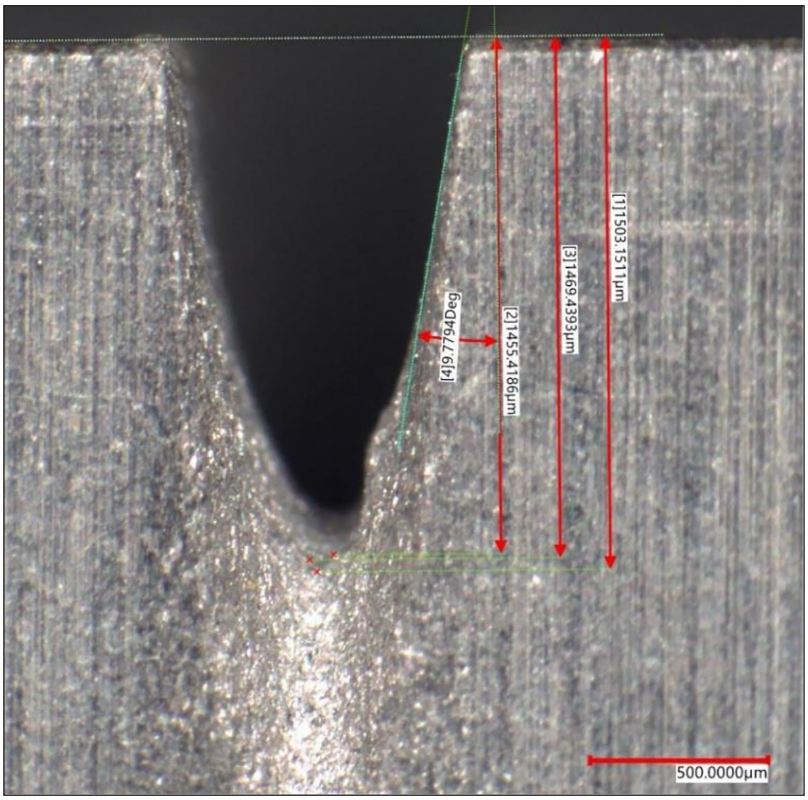

Figure 2. Photo taken with an FVM demonstrating the measurement method

RESULTS AND DISCUSSION

The results of the experimental study provide a detailed analysis of the effects of varying process parameters on the depth of penetration and kerf taper angle during AWJ machining of WNiFe tungsten alloy. Table 2 presents the geometric measurements of the machined grooves, including the depth of penetration and kerf taper angle, under different combinations of jet pressure, traverse speed, and abrasive mass flow rate.

Upon receiving the results of the experiments, statistical analysis was carried out, including

Table 2. Experimental results

No.	p [MPa]	v [mm/min]	m_a [g/s]	Depth [µm]	Angle [deg.]
1	150	225	2	661.3	19.8
2	250	300	3	1063.7	12.6
3	250	225	2	1171.6	9.7
4	200	150	2	1509.6	9.1
5	200	150	4	2309.2	7.0
6	200	225	3	1139.8	10.0
7	250	225	4	1692.1	7.6
8	200	225	3	1292.8	10.0
9	150	150	3	1235.8	11.5
10	150	225	4	1233.9	12.8
11	200	300	2	669.0	14.8
12	200	300	4	1161.8	9.8
13	150	300	3	717.4	15.2
14	200	225	3	1328.1	9.9
15	250	150	3	1997.2	7.8

marginal average analysis and the generation of response surfaces that illustrate the relationships between the dependent and independent variables. The analysis of marginal means is a crucial step in understanding how different process parameters influence the outcomes of the experiments. By examining the marginal means, the effect of each independent variable on the dependent variables can be isolated and evaluated, without the interference of other factors. This method facilitates the identification of the most significant parameters that impact the machining process, leading to optimized settings for enhanced performance.

This study focuses on the depth of the grooves and the kerf angle as the dependent variables. The independent variables under consideration are jet pressure, traverse speed, and abrasive mass flow rate. The analysis of marginal means provides insights into how each factor influences the machining outcomes. The deviation bars in the graphs represent the standard errors of the means, calculated using the mean square errors for each case separately. This helps quantify the data's variability and ensures a clear understanding of the results' reliability. Figure 3 shows the marginal means for the dependent variable, groove depth, and kerf taper angle, concerning the independent variables.

The third graph illustrates the effect of jet pressure on the grooves' depth. The depth increases as the jet pressure rises from 150 MPa to 250 MPa [22]. Higher jet pressures result in more forceful impacts of abrasive particles on the material surface, thereby increasing the penetration depth. The confidence intervals show that the data points are reliable, and the trend is clear. The groove depth increases significantly as the jet pressure increases, but the increase is not linear, as indicated by the percentage increases of 30% and 50% when moving from 150 MPa to 200 MPa and 250 MPa, respectively. This suggests a potentially exponential relationship between jet pressure and groove depth. Higher jet pressures enhance the kinetic energy of the abrasive particles, resulting in more aggressive material removal. This increased energy allows the abrasive particles to penetrate deeper into the tungsten alloy, creating deeper grooves. Figure 3b shows the correlation between jet pressure and the inclination of the groove's wall. As the jet pressure increases from 150 MPa to 250 MPa, the angle decreases. Higher jet pressures result in more forceful impacts of abrasive particles on the material surface, which enhances the removal of material at the edges and results in steeper wall angles. The error bars indicate the variability of the data points, providing an understanding of the reliability of the trends observed in the graphs. This trend highlights the need to carefully control jet pressure to achieve the desired wall angle, as excessively high pressures could lead to overly steep cuts, which may not be desirable for certain applications. According to the research, waterjet pressure significantly impacts the material removal rate (MRR) during abrasive waterjet machining (AWJM). Optimizing this parameter is crucial for enhancing the efficiency of the process [23].

The effect of traverse speed on the grooves' depth has been illustrated in Figure 4. As the traverse speed increases from 150 mm/min to 300 mm/min, the depth of the grooves decreases [24]. Higher traverse speeds reduce the exposure time of the jet on a specific area, leading to

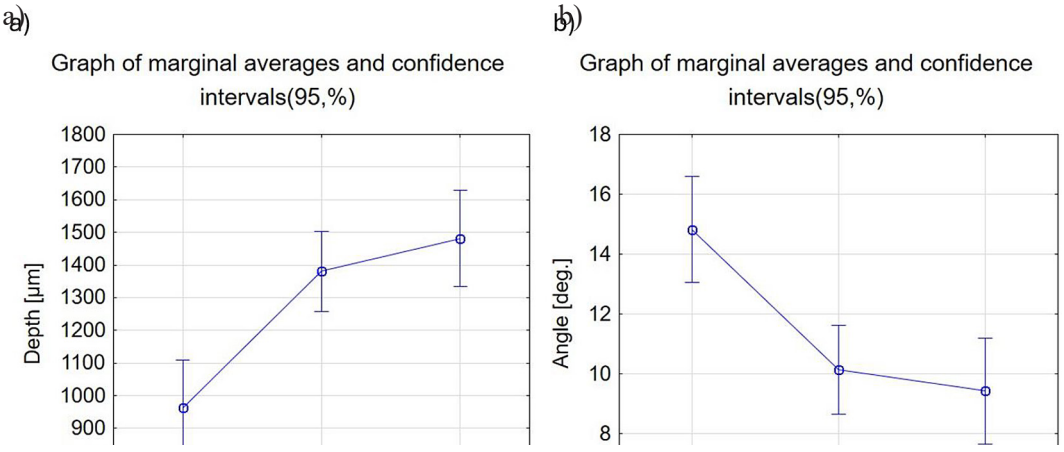

Figure 3. Graph displaying results of analysis of marginal averages for (a) penetration depth and pressure, and (b) penetration depth and taper kerf angle on the right

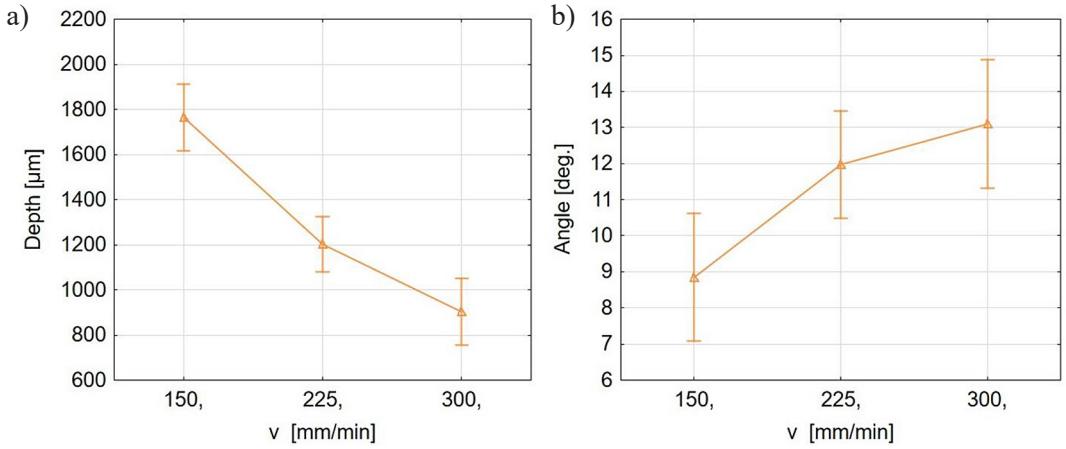

Figure 4. Graph displaying results of analysis of marginal averages for (a) penetration depth, and (b) taper kerf angle in comparison to feed rate

less material being removed and resulting in shallower grooves [25]. The confidence intervals indicate that the data points are reliable and the trend is clear. The decrease in groove depth is significant, showing a substantial reduction in material removal rate with increasing traverse speed. This suggests that slower traverse speeds allow more effective energy transfer from the abrasive particles to the material, thereby increasing penetration depth. However, slower speeds may also reduce the overall machining efficiency by increasing the time required for processing. Figure 4, on the right, depicts the effect of traverse speed on the wall angle of the grooves. As the traverse speed increases from 150 mm/min to 300 mm/min, the wall angle increases. Higher traverse speeds reduce the exposure time of the jet on a specific area, leading to less material being removed at the edges and resulting in larger wall angles. This increase in wall angle with higher traverse speeds suggests that slower speeds allow for more precise and steeper cuts, while higher speeds lead to wider and less defined angles.

The fifth graph illustrates the effect of abrasive mass flow rate on the grooves' depth. As the abrasive mass flow rate increases from 2 g/s to 4 g/s, the depth of the grooves increases significantly [24]. Higher abrasive flow rates result in a greater number of abrasive particles impacting the material surface, thereby enhancing material removal and increasing penetration depth. The substantial increase in groove depth with higher abrasive flow rates suggests that more abrasive particles lead to more effective energy transfer to the material, resulting in deeper grooves [26]. However, while increasing the abrasive mass flow rate enhances the depth of grooves, it also poses challenges in terms of material wear and operational cost. In the graph (Figure 5b), the impact of the

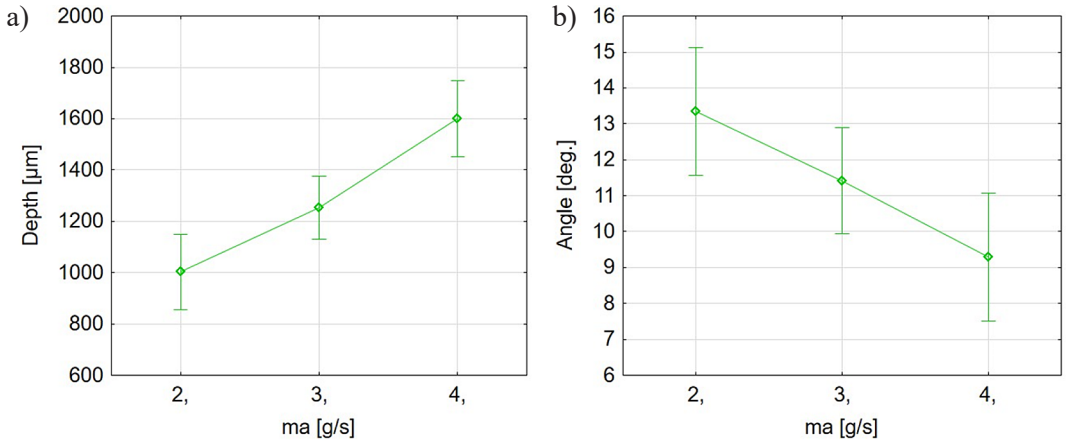

Figure 5. Graph displaying results of analysis of marginal averages for (a) penetration depth and abrasive mass flow rate, (b) Kerf taper angle and abrasive mass flow rate

abrasive mass flow rate on the wall angle of the grooves can be observed. The wall angle decreases significantly as the abrasive mass flow rate increases from 2 g/s to 4 g/s. Higher abrasive flow rates result in more abrasive particles impacting the material surface, creating a steeper cut and reducing the kerf angle. This reduction in inclination angle with higher abrasive flow rates suggests that more abrasive particles lead to more effective material removal at the edges, creating sharper angles.

The following image, captured using a Phenom XL scanning electron microscope (SEM), illustrates the difference in surface quality between grooves 3 and 5, which were machined under different parameters. The SEM images were captured with a field width (FW) of 518 micrometres, using a high voltage (HV) of 15 kV, at a working distance (WD) of 9.797 mm, and under a chamber pressure (Pres.) of 0.1 MPa. These parameters were selected to optimize resolution. Groove 3 was processed at 250 MPa, 225 mm/min, and 2 g/s, while groove 5 was processed at 200 MPa, 150 mm/min, and 4 g/s. The image on the left, where higher pressure and traverse speed but lower abrasive mass flow were used, shows shallower and less distinct grooves formed by the abrasive particles. This indicates that a longer exposure time per unit area and a higher abrasive mass flow can lead to increased surface roughness and more efficient material removal, as more material is cut by individual abrasive particles. The reason for this is that the particles impact perpendicularly to the bottom of the groove. In case the material is not being milled, but cut in its entirety, lower feed rates have a positive effect on surface quality [27]. It can be observed that with higher pressure, the surface becomes smoother, and the grains gradually disappear, suggesting that increased pressure results in a more evenly ground surface

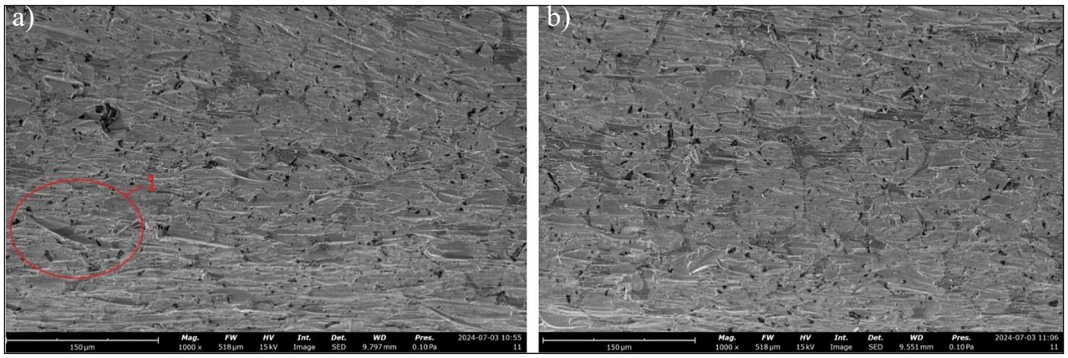

Figure 6. Images of grooves (a) number 3 and (b) number 5 were captured using a scanning electron microscope (SEM) at 1000x magnification

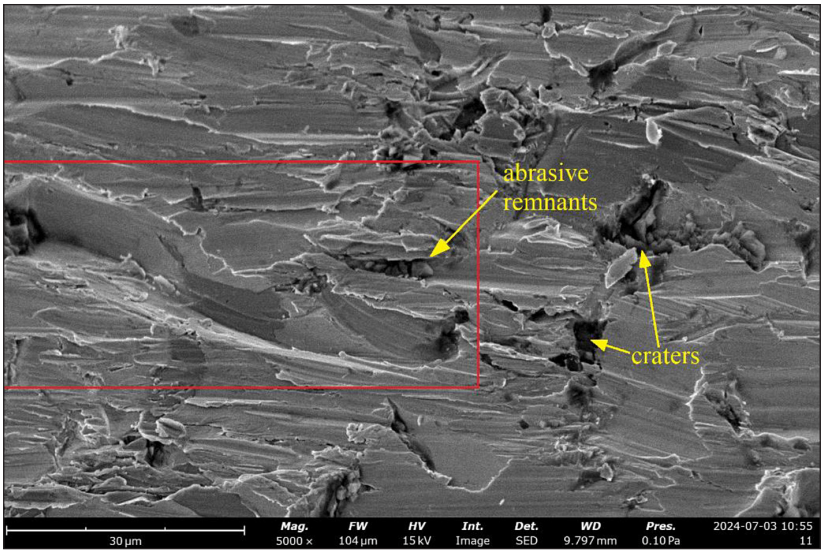

Figure 7. Image of the surface of the fifth groove was captured using SEM at 5000x magnification

and better cutting quality [28]. Additionally, the image below (Figure 7) displays a 5000x magnification of a groove (reference number 1 shown in Figure 6 on the left) formed by the material cutting mechanism of abrasive particles (marked with a red frame in the photo below), providing a better understanding of the material removal process in AWJ machining.

During abrasive waterjet (AWJ) machining, the material removal process involves the impact of high-velocity abrasive particles on the surface, leading to mechanisms such as microcutting, microcracking, and spallation. The rapid stress application causes brittle fracture in the material, resulting in the detachment of small particles. These effects are influenced by process parameters like jet pressure, traverse speed, and abrasive type, impacting the efficiency and quality of the machining process. There are two known types of microcutting mechanisms. On the surfaces of materials processed by the water-abrasive stream, both cutting and abrasion (scratching) effects can be observed. Cutting is caused by abrasive grains with sharp, irregular edges, while material removal by abrasion occurs with oval grains. The rotation direction of the grains relative to the material also affects the cutting marks. In Type I, grains rotate in the direction of motion, while in Type II, grains rotate oppositely. Microcutting occurs only at small impact angles of particles on the material. When these angles approach 90°, abrasive particles striking the surface cause transverse cracks, further promoting material damage, especially in brittle materials.

The investigated material is a tungsten alloy, known for its inherent brittleness. During AWJ machining process, the impact of abrasive particles on the surface results in distinctive topographical features. The SEM image reveals darkened structures indicative of craters formed by the impact of these abrasive particles. Additionally, the presence of scratches can be attributed to the material removal process. The topography of the machined surface appears uneven and chaotic, which is typical given the complexity of the erosion process and the varying angles of particle impact. Embedded abrasive remnants can also be observed within the grooves, highlighting the intensity of the AWJ process. The jagged appearance of the material surface is a consequence of both the mechanical properties of the tungsten alloy and the specific machining parameters used. The inherent brittleness of tungsten, combined with the dynamic and multifaceted nature of the AWJ process, contributes to the irregular surface finish. This characteristic roughness is typical of materials subjected to high-energy particle impacts and reflects the challenges in achieving a uniformly smooth surface through AWJ machining.

Zhu et al. [16] investigated the impact of swaging on the microstructure and mechanical properties of the 90W-7Ni-3Fe tungsten alloy. Their findings, while not directly related to AWJ, provide valuable insights that can be applied to understanding the effects of AWJ machining on tungsten alloy structures. The AWJ process causes the formation of craters and scratches on the material's surface. The high dislocation density and presence of subgrain structures, as observed in Zhu et al.'s study, can contribute to more uniform and predictable material removal. The study noted that microstructural changes, such as the pronounced <101> texture in the W phase at the highest deformation level, can influence the material's impact strength. This same texture may affect how abrasive particles interact with the surface during AWJ machining. The impact of abrasive particles during AWJ machining can lead to further increases in dislocation density and subgrain structures, which enhance the material's hardness and strength. However, the intense interaction of abrasive particles can also cause microcracks and material loss, potentially weakening the material. The study's results show that the crack initiation energy decreases with increasing deformation levels, suggesting that the material becomes more brittle. This phenomenon may also be observed during AWJ machining, where the high-energy impact of abrasive particles can lead to faster crack initiation in the deformed material.

CONCLUSIONS

This study analyzed AWJ machining's impact on WNiFe tungsten alloy, focusing on jet pressure, traverse speed, and abrasive mass flow rate:

- jet pressure: Increasing pressure from 150 to 250 MPa enhances groove depth, suggesting a non-linear relationship; higher pressures yield more aggressive material removal but can lead to steeper wall angles;
- traverse speed: higher speeds (150–300 mm/min) reduce groove depth and precision, while slower speeds enhance penetration but lower machining efficiency;

- abrasive mass flow rate: higher flow rates (2–4 g/s) improve material removal but increase wear and costs; they also lead to steeper cuts and reduced kerf angles;
- surface quality: SEM analysis reveals that higher pressures and slower speeds yield smoother surfaces; craters and scratches result from abrasive particle impacts, reflecting the complex erosion process;
- microstructural impact: high dislocation density and subgrain structures, influenced by machining parameters, aid uniform material removal; however, increased dislocation density and pronounced texture can also cause brittleness and faster crack initiation under high-energy impacts.

Optimizing these parameters is crucial for efficient AWJ machining of tungsten alloys, ensuring balanced material removal and surface integrity. Future studies should explore the microstructural evolution during AWJ machining and its implications for wear properties.

REFERENCES

1. Gopichand G., Sreenivasarao M. Multi-response parametric optimisation of abrasive waterjet milling of Hastelloy C-276 SN Applied Sciences, 2020; 2(11): 1764, DOI: 10.1007/s42452-020-03512-5.
2. Karmiris-Obratański P., Kudelski R., Karkalos N.E., Markopoulos A.P. Determination of the correlation between process parameters and kerf characteristics in abrasive waterjet milling of high strength 7075-T6 aluminum alloy Procedia Manufacturing, 2020; 51: 812–817, DOI: 10.1016/j.promfg.2020.10.114.
3. Goutham U., Kanthababu M., Gowri S., Sunilkumar K.R., Mathanraj M., Jegaraj J.R., Balasubramanian R. Condition monitoring of abrasive waterjet milling using acoustic emission and cutting force signals lecture notes on multidisciplinary industrial engineering, Part F, 2019; 162: 153–164, DOI: 10.1007/978-981-32-9417-2_12.
4. Hashish M., Kotchon A., Ramulu M. Status of AWJ machining of CMCS and hard materials INTERTECH 2015 – An International Technical Conference on Diamond, Cubic Boron Nitride and their Applications, 2015.
5. Bergs T., Schüler M., Dadgar M., Herrig T., Klink A. Investigation of waterjet phases on material removal characteristics Procedia CIRP, 2020; 95: 12–17, DOI: 10.1016/j.procir.2020.02.319.
6. Kong M.C., Axinte D., Voice W. Aspects of material removal mechanism in plain waterjet milling on gamma titanium aluminide J. Mater. Process. Technol., 2010; 210(3): 573–584.
7. Huang L., Folkes J., Kinnell P., Shipway P.H. Mechanisms of damage initiation in a titanium alloy subjected to water droplet impact during ultra-high pressure plain waterjet erosion J. Mater. Process. Technol., 2012; 212(9): 1906–1915.
8. Hlaváček P., Valíček J., Hloch S., Greger M., Foldyna J., Ivandić Ž., Sitek L., Kušnerová M., Zeleňák M. Measurement of fine grain copper surface texture created by abrasive water jet cutting Strojarstvo: časopis za teoriju i praksu u strojarstvu, 2009; 51(4): 273–279.
9. Mieszala M., Lozano Torrubia P., Axinte D.A., Schwiedrzik J.J., Guo Y., Mischler S., Michler J., Philippe L. Erosion mechanisms during abrasive waterjet machining: Model microstructures and single particle experiments Journal of Materials Processing Technology, 2017; 247: 92–102, DOI: 10.1016/j.jmatprotec.2017.04.003.
10. Thomas D.J. Characterisation of aggregate notch cavity formation properties on abrasive waterjet cut surfaces. Journal of Manufacturing Processes, 2013; 15(3): 355–363, Cited 7 times. DOI: 10.1016/j.jmapro.2013.02.003.
11. Dhard C.P., Masuzaki S., Naujoks D., Neu R., Nagata D., Khokhlov M. Exposure of tungsten heavy alloys at high thermal loads in LHD Nuclear Materials and Energy, 2024; 38: 101585, DOI: 10.1016/j.nme.2024.101585.
12. Ye L., Han Y., Fan J., Du Z. Fabrication of ultrafine-grain and great-performance W–Ni–Fe alloy with medium W content Journal of Alloys and Compounds, 2020; 846: 156237, DOI: 10.1016/j.jallcom.2020.156237.
13. Skumavc A., Tušek J., Nagode A., Klobčar D. Thermal fatigue study of tungsten alloy WNi28Fe15 cladded on AISI H13 hot work tool steel Surface and Coatings Technology, 2016; 285: 304–311, DOI: 10.1016/j.surfcoat.2015.09.044.
14. Neu R., Maier H., Balden M., Elgeti S., Gietl H., Greuner H., Herrmann A., Houben A., Rohde V., Sieglin B., Zammuto I. Investigations on tungsten heavy alloys for use as plasma facing material Fusion Engineering and Design, 2017; 124: 450–454, DOI: 10.1016/j.fusengdes.2017.01.043.
15. Žuna Š., Alibašić Z., Imamović A. Investigation of properties of tungsten heavy alloys for special purposes lecture notes in networks and systems, LNNS, 2022; 472: 283–288, DOI: 10.1007/978-3-031-05230-9_32.
16. Zhu W., Liu W., Ma Y., Meng S., Wang J., Duan Y., Cai Q., Influence of microstructure on crack initiation and propagation behavior in swaged tungsten heavy alloy during Charpy impact process Materials Science and Engineering: A, 2023; 862: 144219, DOI: 10.1016/j.msea.2022.144219.

17. Kumar, K. Ravi, V.S. Sreebalaji, and Pridhar T. Characterization and optimization of abrasive water jet machining parameters of aluminium/tungsten carbide composites Measurement 2018; 117: 57–66.
18. Wang, Y., Wang, L., Zhang, X. Modeling of processing parameters for the cutting of rolled tungsten plates via abrasive water jet AIP Advances, 2022; 12(9).
19. Begic-Hajdarevic, D., Bijelonja, I. Laser beam machining of tungsten alloy: experimental and numerical analysis Metals, 2022; 12(11), 1863.
20. Wang, Y., Wang, L., Zhang, X., Mou, N., Yao, D. Cutting of tungsten plate for fusion device via premixed abrasive water jet Fusion Engineering and Design, 2020; 159: 111790.
21. Karkalos N., Muthuramalingam, T., Karmiris-Obratański P. Evaluation of the feasibility of the prediction of the surface morphologiesof AWJ-Milled pockets by statistical methods based on multiple roughness indicators surfaces. 2024; 7: 340–357. DOI: 10.3390/surfaces7020021.
22. Karmiris-Obratański P., Karkalos N.E., Kudelski R., Papazoglou E.L., Markopoulos A.P. On the effect of multiple passes on kerf characteristics and efficiency of abrasive waterjet cutting. Metals, 2021; 11(1): 74; DOI: 10.3390/met11010074.
23. Manoj M., Jinu G. R., Muthuramalingam T. Multi response optimization of AWJM process parameters on machining TiB2 particles reinforced Al7075 composite using Taguchi-DEAR Methodology Silicon, 2018; 10: 2287–2293. DOI: 10.1007/s12633-018-9763-x.
24. Karkalos N.E., Karmiris-Obratański P., Kudelski R., Markopoulos A.P. Experimental study on the sustainability assessment of AWJ machining of Ti-6Al-4V using glass beads abrasive particles Sustainability, 2021; 13(16): 8917. DOI: 10.3390/su13168917.
25. Muthuramalingam T., Swaminathan V., Paramasivam V.K., Thangamani G., Mohamed M. Multi criteria decision making of abrasive flow oriented process parameters in abrasive water jet machining using taguchi–DEAR methodology. Silicon, 2018; 10. DOI: 10.1007/s12633-017-9715-x.
26. Muthuramalingam T., Ahmadein M., Alsaleh N., Elsheikh A. Optimization of abrasive water jet machining of SiC reinforced aluminum alloy based metal matrix composites using taguchi-DEAR. Materials, 2021. DOI: 10.3390/ma14216250.
27. Akkurt A., Kulekci M.K., Seker U., Ercan F. Effect of feed rate on surface roughness in abrasive waterjet cutting applications Journal of Materials Processing Technology, 2004; 147(3): 389–396.
28. Nie, B.S., Zhang, M., Meng, J.Q., Wang, H., Zhang, R.M. Characteristic analysis of metal trough faces cut by pre-mixed abrasive waterjet Applied Mechanics and Materials, 2011; 63: 740–744.